8062 *Biochemistry* **2009,** *48,* 8062–8069
DOI: 10.1021/bi9008962

BIOCHEMISTRY
including biophysical chemistry & molecular biology
Article

Effect of the Redox-Dependent Ionization State of the Heme Propionic Acid Side Chain on the Entropic Contribution to the Redox Potential of *Pseudomonas aeruginosa* Cytochrome c_{551}[†]

Shin-ichi Mikami, Hulin Tai, and Yasuhiko Yamamoto*

Department of Chemistry, University of Tsukuba, Tsukuba 305-8571, Japan

Received May 27, 2009; Revised Manuscript Received July 22, 2009

ABSTRACT: The thermodynamic properties of the redox potentials (E_m) of *Pseudomonas aeruginosa* cytochrome c_{551} (PA) and its mutants possessing a variety of pK_a values for the heme 17-propionic acid side chain, which ranged from ~5 to ~8, have been investigated to elucidate the role of ionization of the heme side chain in the E_m control. Since the pK_a values of the heme 17-propionic acid side chains of the oxidized and reduced forms of PA are 5.9 ± 0.2 and 7.0 ± 0.2, respectively [Takayama, S. J., Mikami, S., Terui, N., Mita, H., Hasegawa, J., Sambongi, Y., and Yamamoto, Y. (2005) *Biochemistry 44*, 5488−5494], the ionization state of the heme 17-propionic acid side chain at physiological pH depends on the oxidation state of the protein. This redox-dependent ionization state of the heme 17-propionic acid side chain was found to have a large effect on the entropic contribution (ΔS) to the E_m value. The magnitude of the E_m control through the ΔS value due to the redox-dependent ionization state of the heme 17-propionic acid side chain was shown to be about 170 mV and hence is considerably larger than that through the enthalpic contribution (ΔH) to the E_m value due to stabilization of the cationic ferriheme in the oxidized protein through partial neutralization of its positive charge by the heme 17-propionate side chain, i.e., about 60 mV [Takayama, S. J., Mikami, S., Terui, N., Mita, H., Hasegawa, J., Sambongi, Y., and Yamamoto, Y. (2005) *Biochemistry 44*, 5488−5494]. The present study revealed that the heme 17-propionic acid side chain of the protein plays a pivotal role in the E_m control of the protein.

Understanding the relationship between the functions and structures of redox active proteins is fundamental and important for extending our knowledge on biological systems. To accomplish this, various studies have been carried out on mono heme class I cytochrome *c* (cyt *c*),[1] because cyt *c* is one of the ideal proteins for elucidating the relationship between the functions and structures of biomolecules (*1*−*9*). Cyts *c* exist in most living organisms, participating in important reactions such as ATP synthesis (*10*), nitrogen fixing (*11*), and apoptosis (*12*, *13*). The redox function of cyts *c* is generally evaluated on the basis of the redox potential (E_m), which can be readily and accurately measured through electrochemical techniques (*14*−*18*). In addition, for structural studies on the proteins, taking advantage of the physicochemical properties characteristic of heme, detailed characterization of their structures in solution has been carried out by means of a variety of spectroscopic techniques (*1*, *2*).

Pseudomonas aeruginosa cytochrome c_{551} (PA) (*19*) and *Hydrogenobacter thermophilus* cytochrome c_{552} (HT) (*20*) are homologous cyts *c* that exhibit 56% homology in primary structure, and their protein folding is almost identical (*19*, *21*). While their structures are highly alike, there is a difference of 60 mV in the E_m value between them, i.e., the E_m values of PA and HT at pH = 6.0 are 303 and 243 mV, respectively (*22*). Thermodynamic studies on their E_m values revealed that the E_m difference arises from both enthalpic (ΔH) and entropic (ΔS) contributions (*22*). Hence, elucidation of the structural factors responsible for the differences in the ΔH and ΔS values between the two proteins is expected to contribute to understanding of the relationship between the functions and structures of cyts *c*. Through studies on PA, HT, and their various mutants, we have revealed that the stabilities of both heme axial coordinations and the hydrophobic core around the heme (*22*−*24*), ionization of the heme 17-propionic acid side chain (*23*), and orientation of polar groups in close proximity to the heme (*25*) control the ΔH value. These findings have been successfully utilized to tune the E_m values of these proteins by means of protein engineering (*23*−*25*). Compared with the knowledge on control of the ΔH value, the molecular mechanism responsible for control of the ΔS value largely remains to be explored, although the protein dynamics and the reorganization effect of water molecules have been proposed to contribute to control of the ΔS value (*26*−*29*).

In this study, we have investigated the effects of ionization of the heme propionic acid side chains of the proteins on the ΔS value. Heme in cyt *c* possesses two propionic acid side chains at positions 13 and 17 (Figure 1). It has been shown that the E_m value of the protein is significantly affected by the ionization states of the heme side chains (*30*−*32*). According to the X-ray structure of PA (*19*) (Figure 1A), the heme 17-propionic acid side chain is buried in the protein matrix and is proposed to be hydrogen-bonded to the side chains of R47 and W56 (Figure 1B),

[†]This work was supported by MEXT, the Yazaki Memorial Foundation for Science and Technology, and the NOVARTIS Foundation (Japan) for the Promotion of Science.

*Corresponding author. Phone: +81-29-853-6521. Fax: +81-29-853-6521. E-mail: yamamoto@chem.tsukuba.ac.jp.

[1]Abbreviations: cyts *c*, cytochromes *c*; E_m, redox potential; PA, *Pseudomonas aeruginosa* cytochrome c_{551}; HT, *Hydrogenobacter thermophilus* cytochrome c_{552}; T_m, denaturation temperature; CV, cyclic voltammetry; δ−pH plots, plots of observed shifts of heme methyl proton signals of proteins against pH; E_m−pH plots, plots of redox potentials of proteins against pH.

 Published on Web 07/23/2009

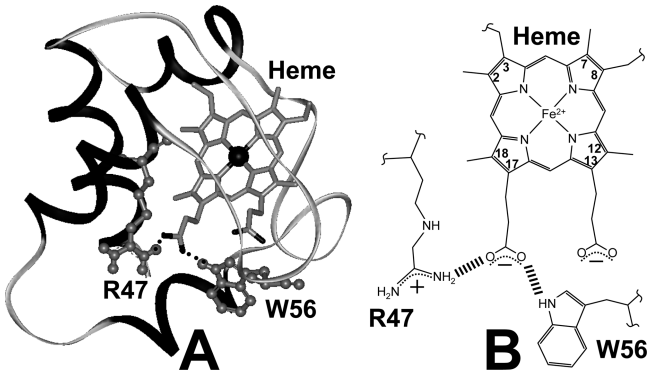

FIGURE 1: (A) Schematic representation of the structure of *P. aeruginosa* cytochrome c_{551} (PA) (*19*) and the locations of heme and amino acid residues R47 and W56. The polypeptide chain is illustrated as a ribbon model, and the heme is drawn as a stick model. The two residues are shown as a ball and stick model, and hydrogen bonds between the side chains of the residues and the heme 17-propionic acid side chain are illustrated by a broken line. (B) Schematic drawing of the hydrogen bond network among the heme 17-propionate, R47, and W56 side chains. The hydrogen bonds are represented by bold broken lines.

while the heme 13-propionic acid side chain is largely exposed to the solvent, exhibiting a pK_a value of about 3.5 (*30*). In general, a charged group in a hydrophobic environment inside a protein is unstable and is stabilized through neutralization on electrostatic interaction with nearby polar group(s). It has been proposed that the heme propionate side chain buried in the protein matrix of cyts *c* is hydrogen-bonded to the positively charged side chain of a Lys or Arg residue to lower its pK_a value in order to maintain a constant E_m value throughout the physiological pH range, because the E_m value is affected by ~60 mV upon the ionization of a heme propionic acid side chain (*23*, *30*−*32*). However, the pK_a values for the heme 17-propionic acid side chains of the oxidized and reduced forms of PA, i.e., 5.9 ± 0.2 and 7.0 ± 0.2, respectively, indicated that the electrostatic interaction between the heme 17-propionate and R47 side chains is rather weak, if any (*23*). Considering the pK_a values of the heme 17-propionic acid side chains of the oxidized and reduced PA, it is expected that ionization/deionization of the heme 17-propionic acid/propionate side chain of the proteins is coupled with a change in their oxidation state. This redox-dependent ionization of the heme 17-propionic acid side chain influences the heme environment and hence is expected to contribute to control of the ΔS value.

In order to clarify the effect of the redox-dependent ionization of the heme 17-propionic acid side chain on ΔS control of the protein, we have prepared mutants possessing a variety of pK_a values for this heme side chain. We have previously shown that the F34Y and E43Y mutants of PA, for which amino acid substitutions were selected with reference to the corresponding residues in HT, exhibit pK_a values of <4.5 and 5.0 ± 0.2, respectively, for the oxidized proteins and <5.5 and 6.0 ± 0.2, respectively, for the reduced ones (*23*). Thus the F34Y and E43Y mutations of PA resulted in remarkable lowering of the pK_a value of the heme 17-propionic acid side chain. In this study, we have carried out R47L and W56F mutations of PA in order to obtain mutants with pK_a values largely different from that of the wild-type protein. As described above, the heme 17-propionic acid side chain of PA was proposed to be hydrogen-bonded to the side chains of both R47 and W56, and hence the removal of these hydrogen bond donors by the mutations is expected to lead to a large change in alteration of the electrostatic environment around the heme 17-propionic acid side chain in the protein, which in turn changes the pK_a value.

In the present study, we have examined, based on characterization of the pH- and temperature-dependent profiles of the E_m values of PA and its F34Y, E43Y, R47L, and W56F mutants, the relationship between the pK_a values of the heme 17-pripionic acid side chains of the proteins and the ΔS values in order to elucidate the effects of the redox-dependent ionization state of the heme 17-propionic acid side chain on the ΔS control. Since the oxidized R47L and W56F exhibited pK_a values of 6.7 ± 0.2 and 7.9 ± 0.2, respectively, the removal of the hydrogen bond between the heme 17-propionic acid and R47 (or W56) side chains (heme−R47 (or W56) H-bond) was found to increase the pK_a value of the heme 17-propionic acid side chain. Comparative study of the ΔS values of the proteins of which the heme 17-propionic acid side chains exhibit pK_a values ranging from ~5 to ~8 revealed a clear relationship between the ΔS and pK_a values of the proteins in such a manner that a protein with a pK_a value closer to the pH condition used for the ΔS measurement exhibits a larger ΔS value. This finding not only unequivocally demonstrated that the redox-dependent ionization state of the heme 17-propionic acid side chain contributes to the ΔS control but also provided novel insights for tuning of the E_m value of the protein through the relationship between the ΔS and pK_a values by protein engineering.

MATERIALS AND METHODS

Protein Samples. The wild-type PA and mutants were produced using *Escherichia coli* and purified as reported previously (*33*, *34*). The oxidized forms of the proteins were prepared by the addition of a 10-fold molar excess of potassium ferricyanide. For NMR samples, the proteins were concentrated to about 1 mM in an ultrafiltration cell (YM-5, Amicon), and then 10% ^2H_2O was added to the protein solutions. The pH of each sample was adjusted using 0.2 M KOH or 0.2 M HCl, and the pH was monitored with a Horiba F-22 pH meter with a Horiba type 6069-10C electrode.

^1H NMR. NMR spectra were recorded on a Bruker Avance 600 FT NMR spectrometer operating at the ^1H frequency of 600 MHz. Samples for NMR measurements comprised ~1.0 mM protein in nominal ^1H_2O (~90% ^1H_2O/~10% ^2H_2O), together with 20 mM potassium phosphate buffer, pH 7.0. Typical spectra of the oxidized proteins required a 100 kHz spectral width, 32K data points, a 9 μs 90° pulse, a 1 s recycle time, and ~2K scans, and the water signal was suppressed with a 100 ms presaturation pulse. Chemical shifts are given in parts per million downfield from sodium 2,2-dimethyl-2-silapentane-5-sulfonate with H_2O as an internal reference.

The pH dependence of the chemical shifts of the heme methyl proton signals of the oxidized proteins was analyzed using the following equation in order to estimate the pK_a value of the heme 17-propionic acid side chain:

$$\delta_{obs} = \{\delta_{COOH} + \delta_{COO^-}[10^{(pK_a - pH)}]\}/[1 + 10^{(pK_a - pH)}] \quad (1)$$

where δ_{obs} is the chemical shift of heme methyl proton signal at certain pHs and δ_{COOH} and δ_{COO^-} are those where the heme 17-propionic acid side chain is fully protonated and ionized, respectively.

Cyclic Voltammetry. The procedures used for the measurement of cyclic voltammograms of the proteins were essentially the

same as those described previously (*22*, *35*−*37*). Cyclic voltammetry (CV) experiments were performed with a potentiostat−galvanostat PGSTAT12 (Autolab, The Netherlands). A gold electrode treated with 4,4′-dipyridyl disulfide just before use was employed as the working electrode. An Ag|AgCl electrode in a saturated NaCl solution and a Pt wire were employed as the reference and counter electrodes, respectively. The potential sweep range was from +350 to −150 mV vs the Ag|AgCl electrode in a saturated NaCl solution with the scan rate of 20 mV s^{-1}. All potentials are referenced to the standard hydrogen electrode. The protein concentration was about 0.5 mM in 20 mM phosphate buffer, pH 4.0−9.0, and 0.1 M $NaClO_4$. All experiments were performed at 25 °C under a nitrogen atmosphere. The anodic to cathodic peak current ratios obtained at various potential scan rates (1−100 mV s^{-1}) were all ∼1. Both the anodic and cathodic peak currents increased linearly as a function of the square root of the scan rate in the range up to 100 mV s^{-1}. The anodic and cathodic peak separations of the scan rate in the range up to 100 mV s^{-1} were approximately 100 mV. Thus, PA and its mutants exhibit quasi-reversible redox processes.

The pH profiles of the E_m values were analyzed using the following equation in order to estimate the pK_a values of the heme 17-propionic acid side chains in the reduced and oxidized proteins, K_{red} and K_{ox}, respectively (*38*):

$$E_m = E_{m(H)} + (RT/nF)\log\{(K_{red} + [H^+])/(K_{ox} + [H^+])\} \quad (2)$$

where $E_{m(H)}$ represents the E_m value of protein with the fully protonated heme 17-propionic acid side chain, R is gas constant, T is absolute temperature, n is the number of electrons transferred by the redox couple, and F is the Faraday constant. The equation was used to generate the theoretical curve by optimizing pK_{red} and pK_{ox} to give the best fit to the experimental data.

Thermodynamic parameters, i.e., ΔH and ΔS, were calculated from the E_m values measured over the temperature range of ∼10 to ∼60 °C. The ΔH value was obtained from the slope of the plots of E_m/T against $1/T$, according to the Gibbs−Helmholtz equation, i.e., $\Delta G = \Delta H - T\Delta S = -nFE_m$. The ΔS value was obtained from the slope of the plots of E_m against T. The experimental errors for the ΔH and ΔS values of the proteins except the R47L mutant were ±2 kJ mol^{-1} and ±3 J K^{-1} mol^{-1}, respectively. Due to the poor electrochemical response, the E_m value of R47L was only obtained in the temperature range of 25−45 °C, and hence the experimental errors for the ΔH and ΔS values of the R47L mutant were ±7 kJ mol^{-1} and ±10 J K^{-1} mol^{-1}, respectively.

Circular Dichroism Spectroscopy. Circular dichroism (CD) spectra were recorded on a JASCO J-820 spectrometer over the spectral range of 200−300 nm and in the temperature range of 30−130 °C, using an airtight pressure-proof cell compartment with quartz windows, as described previously (*39*).

RESULTS

^{1}H NMR Spectra of PA and Its Mutants and Their pH Profiles. We first analyzed the effects of the amino acid substitutions on the heme active site structure of the proteins by paramagnetic ^{1}H NMR. The 600 MHz ^{1}H NMR spectra of the oxidized forms of PA and the mutants at pH 6.0 and 25 °C are compared with each other in Figure 2. The spectra of oxidized PA, F34Y, and E43Y have been reported previously (*23*). The heme active site structures of the proteins have been shown to be sensitively manifested in paramagnetic shifts of the heme peripheral and Fe-bound Met side chain proton signals of the oxidized proteins (*40*−*42*). The spectral patterns observed for all the proteins were essentially similar to each other, indicating that the structural properties of the heme active site were not significantly affected by the amino acid substitution(s) introduced into the mutants. Spectra of the proteins at various pH values were recorded (see the Supporting Information), and the pH profiles of the observed shifts of the heme methyl proton signals (δ−pH plots) for the R47L and W56F mutants are compared with those of the oxidized PA, F34Y, and E43Y previously reported (*23*) in Figure 3. The δ−pH plots of the proteins have been shown to reflect the pK_a value of the heme 17-propionic acid side chain (*23*, *30*, *32*). The pK_a values of 6.7 ± 0.2 and 7.9 ± 0.2 were determined from the δ−pH plots for the oxidized R47L and W56F mutants, respectively. Since the oxidized PA, F34Y, and E43Y (*23*) exhibit values of 6.1 ± 0.2, 5.0 ± 0.2, and < 4.5, respectively (*23*), the pK_a value of the heme 17-propionic acid side chain was found to increase with removal of the heme−R47 and heme−W56 H-bonds.

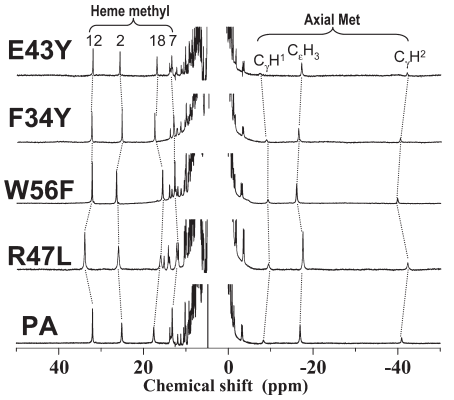

FIGURE 2: 600 MHz ^{1}H NMR spectra of the oxidized forms of PA, R47L, W56F, F34Y, and E43Y in 90% H_2O/10% ^2H_2O, pH 6.0, at 25 °C. The heme methyl and axial Met side-chain proton signals are indicated with the spectra, and the corresponding resonances are connected by broken lines. The spectra for PA, F34Y, and E43Y were reported previously (*23*).

pH Profiles of the E_m Values of the R47L and W56F Mutants. We next measured the E_m values of the R47L and W56F mutants at various pHs, the pH profiles of the obtained values (E_m−pH plots) for the proteins, together with those for PA, F34Y, and E43Y for comparison, being shown in Figure 4A. The E_m values of R47L and W56F at pH 6.0 were 265 and 280 mV, respectively (Table 1), and exhibited a negative shift of about 40 mV with increasing pH to 9. The fitting of the E_m−pH plots to the Nernst equation (*43*) yielded pK values of 6.9 ± 0.2 and 7.5 ± 0.2 for the oxidized and reduced forms (pK_{ox} and pK_{red}) of the R47L mutant, respectively, and pK_{ox} and pK_{red} values of 7.9 ± 0.2 and 8.4 ± 0.2 for the W56F mutant, respectively (see the Supporting Information). The similarity between the pK_a value of the heme 17-propionic acid side chain, estimated from the δ−pH plots, and the pK_{ox} value, determined from the E_m−pH plots, for the oxidized R47L and W56F mutants confirmed that the E_m values of the proteins are affected by ionization of the heme 17-propionic acid side chain. In order to highlight the differences in the pK value, reflected in the E_m−pH plots, among the proteins, the data were plotted in such a way that the E_m values of R47L and W56F at pH 4.5 and those of F34Y and E43Y at pH 9.0 were normalized to the corresponding values for PA in Figure 4B.

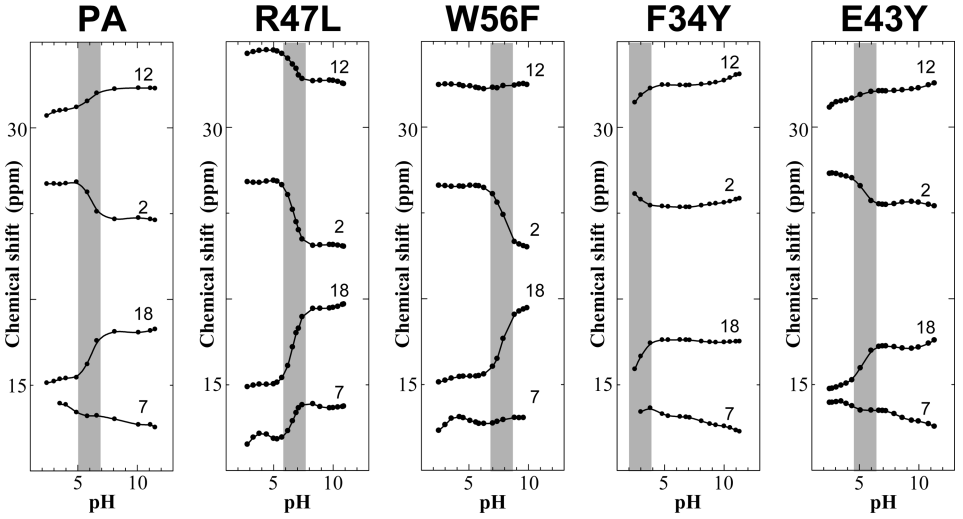

FIGURE 3: pH dependence of the chemical shifts of the heme methyl proton signals of the oxidized forms of PA, R47L, W56F, F34Y, and E43Y in 90% ^1H_2O/10% ^2H_2O at 25 °C. The pH region in which the heme methyl proton signals exhibited large pH-dependent shifts is indicated in gray. The plots for PA, F34Y, and E43Y were reported previously (*23*).

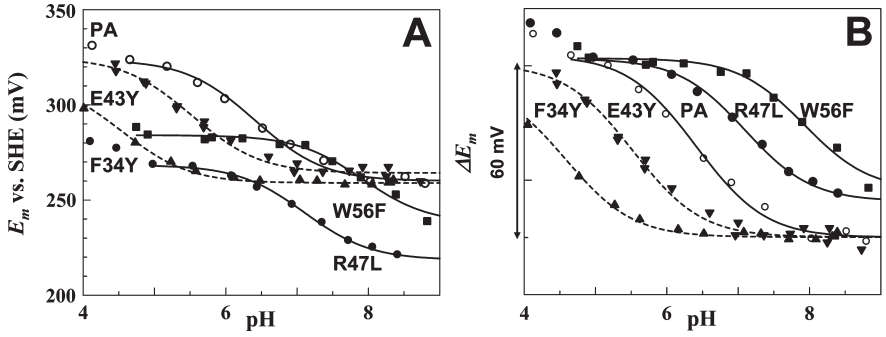

FIGURE 4: (A) Plots of the redox potentials (E_m) against pH for PA (○) and the R47L (●), W56F (■), F34Y (▲), and E43Y (▼) at 25 °C. The plots for PA, F34Y, and E43Y were reported previously (*23*). (B) Fitting of the plots in (A) to the Nernst equation was performed in such a way that the E_m values of PA, F34Y, and E43Y at pH 9.0 were normalized to the corresponding values for PA, in order to compare the pK_a values reflected in the pH profiles of the E_m values.

Table 1: E_m, ΔS, ΔH, T_m, and pK_a Values for PA and Its Mutants

protein	E_m (mV)[a]	ΔS (J K^{-1} mol^{-1})[b]	ΔH (kJ mol^{-1})[b]	T_m (°C)[c]	pK_{ox} (NMR)[d]	pK_{ox} (CV)[e]	pK_{red}(CV)[e]
PA	303[f]	−64.5[f] (−52)	−47[f] (−48)[g]	82.1	6.1[h]	5.9[h]	7.0[h]
R47L	265	−45	−39	75	6.7	6.9	7.5
W56F	280	−36	−38	73	7.9	7.9	8.4
F34Y	254[i]	−42[i] (−45)[g]	−38 (−41)[g]	91	< 4.5[h]	< 4.5[h]	< 5.5[h]
E43Y	285	−92	−55	87	5.0[h]	5.0[h]	6.0[h]

[a] Redox potential determined at pH 6.0 and 25 °C. The experimental error was ±5 mV. [b] The entropic and enthalpic contributions to the E_m value at pH 6.0. The experimental errors for ΔS and ΔH of the proteins except the R47L mutant were ±3 J K^{-1} mol^{-1} and ±2 kJ mol^{-1}, respectively, and those of the R47L mutant were ±10 J K^{-1} mol^{-1} and ± 7 kJ mol^{-1}, respectively. [c] The denaturation temperature of the oxidized protein at pH 7.0 determined through analysis of the temperature dependence of the CD ellipticity at 222 nm. [d] The pK_a value obtained from the pH-dependent shifts of heme methyl proton signals of the oxidized form of the protein. The experimental error was ±0.2. [e] The pK_a values of the oxidized and reduced forms of the protein, pK_{ox} and pK_{red}, respectively, determined from the fitting of the pH profile of the E_m value to the Nernst equation (see the Supporting Information). The experimental error was ±0.2. [f] Taken from ref *24*. [g] The numbers in parentheses indicate the values determined at pH 5.0. The experimental error was ±0.2. [h] Taken from ref *23*. [i] The value was slightly different from that previously reported (*30*) possibly due to the effect of ionic strength on the ΔS value (*47*).

Temperature Dependence of the E_m Values of the R47L and W56F Mutants. We also measured the E_m values of R47L and W56F at pH 6.0 and various temperatures, and the obtained values, together with those of PA, F34Y, and E43Y for comparison, are plotted against temperature (E_m−T plots) in Figure 5. Similarly to the cases of PA, F34Y and E43Y, the E_m−T plots for R47L and W56F each exhibited a straight line (Figure 5). From the E_m−T plots, we estimated the ΔH and ΔS values (Table 1). As listed in Table 1, the ΔS value is more largely affected by the amino acid substitutions introduced into the mutants than the ΔH value is. The proteins could be ranked as W56F < R47L ≈ F34Y < PA < E43Y, in order of increasing absolute ΔS value ($|\Delta S|$) determined at pH 6.0. Comparison of the ΔS and pK_a values for the heme 17-propionic acid side chain of the protein suggested that a protein with a pK_a value closer to pH 6.0 exhibits a larger $|\Delta S|$ value. In fact, the ΔS value of −52 ± 3 J K^{-1} mol^{-1}

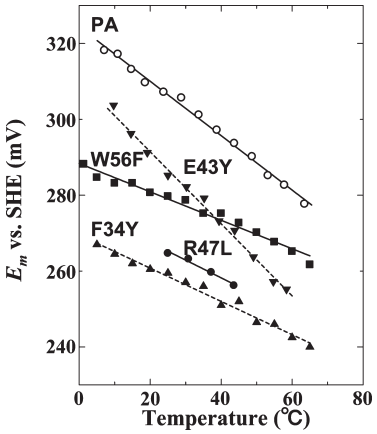

FIGURE 5: Plots of the redox potentials (E_m) against temperature for PA (○) and the R47L (●), W56F (■), F34Y (▲), and E43Y (▼) at pH 6.0. Due to the poor electrochemical response, the E_m value of R47L was only obtained in the temperature range of 25−45 °C.

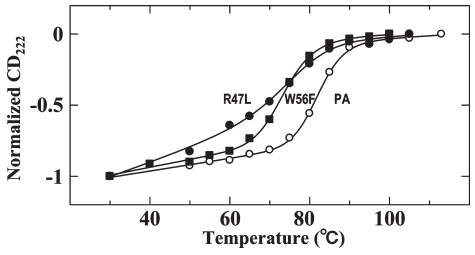

FIGURE 6: Thermal unfolding profiles of the oxidized forms of PA (○), R47L (●), and W56F (■) at pH 7.0.

determined for PA at pH 5.0 was considerably smaller in magnitude than the value at pH 6.0, i.e., -64.5 ± 3 J K^{-1} mol^{-1} (Table 1). On the other hand, the value of -45 ± 3 J K^{-1} mol^{-1} determined for the F34Y mutant at pH 5.0 was essentially equal to the value at pH 6.0, i.e., -42 ± 3 J K^{-1} mol^{-1} (Table 1). These results clearly confirmed the relationship between the ΔS and pK_a values of the proteins in such a manner that a protein with a pK_a value closer to the pH condition used for the ΔS measurements exhibits a larger ΔS value, demonstrating that the redox-dependent ionization of the heme 17-propionic acid side chain significantly contributes to control of the ΔS value.

Thermostability of the Mutants. We finally analyzed the thermostability of the oxidized R47L and W56F mutants through measurement of CD spectra (200−300 nm) in the temperature range of 30−130 °C at pH 7.0. The fractions of the unfolded proteins calculated from the CD ellipticity at 222 nm were plotted against temperature, thermal unfolding profiles for the two mutants being obtained (Figure 6). Similar plots for the oxidized form of PA are also illustrated, for comparison, in Figure 6. The denaturation temperatures (T_m) of R47L and W56F were determined to be 75 and 73 °C, respectively, which were lower than that of PA, i.e., 82 °C (Table 1). The lowering of the T_m value caused by the R47L and W56F mutations can be attributed to removal of the heme−R47 and heme−W56 H-bonds, respectively. These results indicated not only that both the heme−R47 and heme−W56 H-bonds contribute to the stability of the oxidized protein but also that the contribution of the latter H-bond to the protein stability is greater than that of the former one. According to the X-ray crystal structure of PA (*19*), the donor−acceptor distances for the heme−R47 and heme−W56 H-bonds are 0.184 and 0.174 nm, respectively. Therefore, the greater contribution of the heme−W56 H-bond to the protein stability than that of the heme−R47 one is consistent with the higher stability of the latter than that of the former, as expected from their hydrogen bond distances. On the other hand, the T_m values of the F34Y and E43Y mutants, i.e., 91 and 87 °C, respectively, are higher than that of PA, indicating the possible formation of a hydrogen bond between the introduced Tyr residue and the heme 17-propionic acid side chain in the protein.

DISCUSSION

Effect of the Mutations on the Protein Structure. Although the amino acid replacements introduced into the mutants did not significantly change the heme active site structure of PA, as reflected in the similarity of the paramagnetic shift pattern of the heme peripheral and Fe-bound Met side chain proton NMR signals among the oxidized proteins, but induced sizable changes in both the chemical environment around the buried heme 17-propionic acid side chain and thermostability of the protein, as manifested in the pK_a and T_m values, respectively. The pK_a of a titrating group in a protein is sensitively affected by not only its electrostatic environment but also nonelectrostatic interactions such as the amount of water nearby, the extent of burial, and the flexibility of polar side chains around a titrating group, in addition to van der Waals and hydrophobic interactions (*44*). In the case of PA, the pK_a value for the heme 13-propionic acid side chain was reported to be about 3.5 (*30*), the values for the heme 17-propionic side chains in the oxidized and reduced forms being 5.9 ± 0.2 and 7.0 ± 0.2, respectively (*23*). The X-ray crystal structure of PA indicated that the heme 13-propionic acid side chain is largely exposed to the solvent, while the heme 17-propionic acid side chain is buried inside the hydrophobic core of the protein, with the formation of heme−R47 and heme−W56 H-bonds (*19*). The hydrophobic environment around the heme 17-propionic acid side chain and the formation of the hydrogen bond network significantly contribute to the control of its pK_a value, as manifested in the difference in the pK_a value between the heme 13- and 17-propionic acid side chains of PA, as well as the effect of the R47L and W56F mutations on the pK_a value. Consequently, the increase in the pK_a value caused by the R47L and W56F mutations could be attributed primarily to removal of the heme−R47 and heme−W56 H-bonds, respectively, in addition to alteration of the hydrophobic environment around the heme 17-propionic acid side chain exerted by the mutations. The loss of the heme−R47 and heme−W56 H-bonds caused by the R47L and W56F mutations, respectively, is clearly manifested in the lower T_m values for the mutants. Since PA exhibits pK_{ox} and pK_{red} values of 5.9 ± 0.2 and 7.0 ± 0.2, respectively, the electrostatic interaction between the heme 17-propionate and R47 side chains can be considered to be weak, as described previously (*23*). Weak electrostatic interaction between the heme 17-propionate and R47 side chains may appear to be in conflict with rather strong heme−R47 H-bond as manifested in its sizable contribution to the stability of the overall protein structure. Since guanidyl group of the R47 side chain is fully exposed to the solvent (*19*), its positive charge would be stabilized through interaction with solvent molecules, and hence the ionization of heme 17-propionic acid side chain is not largely affected by the positive charge of the R47 side chain even in the presence of the heme−R47 H-bond.

By the way, although both the pK_{ox} and pK_{red} values of the wild-type protein were increased by the R47L and W56F

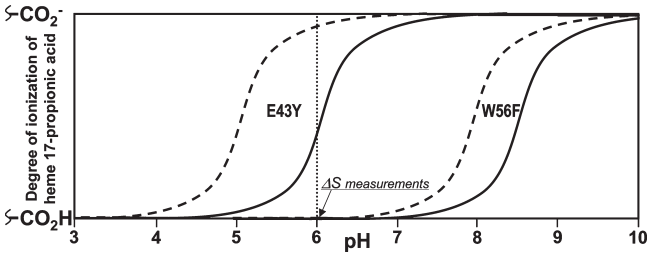

FIGURE 7: Schematic representation of the pH-dependent ionization profiles of the heme 17-propionic acid side chains of E43Y, with pK_{ox} and pK_{red} values of 5.0 ± 0.2 and 6.0 ± 0.2, respectively (left), and W56F, with values of 7.9 ± 0.2 and 8.4 ± 0.2, respectively (right). The profiles of the oxidized and reduced proteins are indicated by broken and solid lines, respectively. The pH value used for the ΔS measurements, i.e., pH 6.0, is indicated by a dotted line. At pH 6.0, the heme 17-propionic acid side chain of the oxidized E43Y is mostly ionized, whereas that of the reduced one is ionized about halfway. Therefore, the ionization state of the heme 17-propionic acid side chain of E43Y is affected by the redox state of the protein. On the other hand, since the heme 17-propionic acid side chains of the oxidized and reduced W56F are mostly protonated, the ionization state of the heme 17-propionic acid side chain of W56F is almost completely independent of the oxidation state of the protein. The redox-dependent ionization state of the heme 17-propionic acid side chain significantly contributes to control of the ΔS value. The study demonstrated that a protein of which the pK_a value is closer to the pH value used for the ΔS measurements exhibits a larger absolute ΔS value.

mutations, the magnitude of the increase for the former value, with a given mutation, was larger than that for the latter, and hence, as a result, the difference between the two values of the mutants became smaller compared with that of the wild-type protein. Thus the effect of the mutation on the pK_a value of the heme 17-propionic acid side chain depends on the oxidation state of the protein, indicating a close mutual interaction between the ionization state of the heme 17-propionic acid side chain and heme iron.

Correlation between the ΔS and pK_a Values for the Heme 17-Propionic Acid Side Chain. As shown in Table 1, the ΔS value determined at pH 6.0 is related to the pK_a value of the heme 17-propionic acid side chain of the protein in such a manner that a protein of which the pK_a value is close to the pH value used for the ΔS measurements exhibits a larger $|\Delta S|$ value. For example, the E43Y mutant with pK_{ox} and pK_{red} values of 5.0 ± 0.2 and 6.0 ± 0.2, respectively (*23*), exhibited a relatively large $|\Delta S|$ value, whereas the F34Y mutant with values of < 4.5 and < 5.5, respectively (*23*), and the W56F mutant with ones of 7.9 ± 0.2 and 8.4 ± 0.2, respectively, exhibited relatively small $|\Delta S|$ values. According to their pK_{ox} and pK_{red} values, under the pH condition used for the ΔS measurements, i.e., pH 6.0, the heme 17-propionic acid side chain of the oxidized E43Y mutant is mostly ionized, whereas that of the reduced one is ionized roughly halfway (Figure 7). Thus, the ionization state of the heme 17-propionic acid side chain of the E43Y mutant at pH 6.0 is affected by the redox state of the protein. On the other hand, at pH 6.0, the heme 17-propionic acid side chains of both the oxidized and reduced forms of the F34Y mutant are mostly ionized, and on the contrary, those of the W56F mutant are mostly protonated. Hence the magnitude of the redox-dependent deprotonation/protonation of the heme 17-propionic acid/propionate side chains in these mutants at this pH value is considerably smaller than that in the E43Y mutant.

In general, the ΔS values of cyts *c* are negative (*5*, *26*, *28*, *45*, *46*), indicating that, with a given protein, the entropy (*S*) of the reduced form is smaller than that of the oxidized one. The redox-dependent *S* value of the protein has been attributed to a difference in structural dynamics near the heme between the two redox states (*28*). The presence of a negative charge resulting from deprotonation of the heme 17-propionic acid side chain in the protein is thought to lead to destabilization of the hydrophobic core of the protein and hence weakening of the packing of the heme pocket, which in turn results in an increase in the *S* value of the protein. In the case of the W56F mutant, the heme 17-propionic acid side chains of both the redox forms are not ionized at pH 6.0, and hence, due to the absence of redox-dependent ionization of the heme 17-propionic acid side chain, this mutant exhibited a relatively small $|\Delta S|$ value of 36 J mol^{-1} K^{-1}. A similarly small $|\Delta S|$ value of 42 J mol^{-1} K^{-1} for the F34Y mutant can also be attributed to the absence of redox-dependent ionization of the heme 17-propionic acid side chain, because the heme side chains of both the oxidized and reduced forms of the protein are mostly ionized at pH 6.0. Furthermore, the similarity in the $|\Delta S|$ value between the W56F and F34Y mutants suggested that the effect of the ionization state of the heme 17-propionic acid side chain on the *S* value is almost completely independent of the oxidation state of the protein. Therefore, a ΔS value of ~ -40 J mol^{-1} K^{-1} is likely to be the upper limit of the values attainable within the framework of the present protein structure and is equivalent to an E_m value of ~ -110 mV at room temperature. On the other hand, the large $|\Delta S|$ value of 92 J mol^{-1} K^{-1} for the E43Y mutant is attributed to the redox-dependent ionization state of the heme 17-propionic acid side chain. Thus, ionization of the heme 17-propionic acid side chain of the protein plays a significant role in E_m control through its effect on the ΔS value. By the way, although the pK_{red} value of the E43Y mutant and the pK_{ox} value of the wild-type PA are similar to each other, there is a large difference in the ΔS value, i.e., $\sim$30 J mol^{-1} K^{-1}, between the two proteins. This result suggested that the effect of the ionization of the heme 17-propionic acid side chain on the *S* value of the protein depends crucially on the local environment around the heme side chain.

Effect of Ionization of the Heme 17-Propionic Acid Side Chain of the Protein on E_m Control. The E_m value of the protein has been shown to exhibit a negative shift of $\sim$60 mV upon ionization of the heme 17-propionic acid side chain (*23*) (Figure 4A). This E_m change has been explained in terms of the stabilization of the cationic ferriheme in the oxidized protein, relative to the neutral ferroheme in the reduced one, in the hydrophobic environment of the heme active site through partial neutralization of its positive charge by the heme 17-propionate side chain (*23*). Thus, the ionization state of the heme 17-propionic acid side chain of the protein enthalpically controls the E_m value.

As described above, the redox-dependent ionization state of the heme 17-propionic acid side chain of the protein contributes to E_m control through its effect on the ΔS value. The difference in the $|\Delta S|$ value between W56F and E43Y, i.e., 56 J mol^{-1} K^{-1}, would account for the net effect of the redox-dependent ionization of the heme 17-propionic acid side chain of the protein on the ΔS value and was larger than the $|\Delta S|$ value of $\sim$40 J mol^{-1} K^{-1} due to the differences in intrinsic dynamical properties between the two different redox forms of the protein. The $|\Delta S|$ value of 56 J mol^{-1} K^{-1} due to the redox-dependent ionization of the heme 17-propionic acid side chain is equivalent to an E_m change of $\sim$170 mV at room temperature, and hence, depending upon

the pK_a value of the heme 17-propionic acid side chain, the effect of its ionization on the ΔS value could be much larger than that on the ΔH one.

Characterization of the thermodynamic properties of the E_m values of PA and its mutants possessing a wide range of pK_a values for the heme 17-propionic acid side chain, i.e., pK_a = ~5 to ~8, revealed that the redox-dependent ionization state of the heme 17-propionic acid side chain is a major determinant of the ΔS value. The ΔS value determined by the redox-dependent ionization state of the heme 17-propionic acid side chain of the protein was found to be larger than that due to the differences in intrinsic dynamical properties between the two different redox states of the protein. Furthermore, the magnitude of the E_m control through the ΔS value determined by the redox-dependent ionization state of the heme 17-propionic acid side chain was found to be considerably larger than that through the previously reported ΔH value due to the selective stabilization of the cationic ferriheme in the oxidized protein through partial neutralization of its positive charge by the heme 17-propionate side chain. Thus, the heme 17-propionic acid side chain of the protein plays a pivotal role in the E_m control of the protein. These findings provide novel insights into the functional control of cyts *c*, which could be utilized for tuning of the E_m values of the proteins through designing of the chemical environment around the heme 17-propionic acid side chain by means of protein engineering.

ACKNOWLEDGMENT

The ^{1}H NMR spectra were recorded on a Bruker AVANCE-600 spectrometer at the Chemical Analysis Center, University of Tsukuba.

SUPPORTING INFORMATION AVAILABLE

pH dependence of 600 MHz ^{1}H NMR spectra of the oxidized forms of PA, R47L, W56F, F34Y, and E43Y at 25 °C and analyses of the pH profiles of the E_m values of PA, R47L, W56F, and E43Y at 25 °C. This material is available free of charge via the Internet at http://pubs.acs.org.

REFERENCES

1. Moore, G. R., and Pettigrew, G. W. (1990) Cytochromes c: Evolutionary, structural, and physicochemical aspects, Springer-Verlag, Berlin.
2. Scott, R. A., and Mauk, A. G., Eds. (1996) Cytochrome c: A multidisciplinary approach, University Science Books, Sausalito, CA.
3. Warshel, A., Papazyan, A., and Muegge, I. (1997) Microscopic and semimacroscopic redox calculations: what can and cannot be learned from continuum models. *J. Biol. Inorg. Chem. 2*, 143–152.
4. Gunner, M. R., Alexov, E., Torres, E., and Lipovaca, S. (1997) The importance of the protein in controlling the electrochemistry of heme metalloproteins: methods of calculation and analysis. *J. Biol. Inorg. Chem. 2*, 126–134.
5. Battistuzzi, G., Bellei, M., Borsari, M., Canters, G. W., de Waal, E., Jeuken, L. J., Ronieri, A., and Sola, M. (2003) Control of metalloprotein reduction potential: Compensation phenomena in the reduction thermodynamics of blue copper proteins. *Biochemistry 42*, 9214–9220.
6. Blouin, C., and Wallace, C. J. A. (2001) Protein matrix and dielectric effect in cytochrome *c*. *J. Biol. Chem. 276*, 28814–28818.
7. Springs, S. L., Bass, S. E., and McLendon, G. L. (2000) Cytochrome b_{562} variants: A library for examining redox potential evolution. *Biochemistry 39*, 6075–6082.
8. Reedy, C. J., and Gibney, B. R. (2004) Heme protein assemblies. *Chem. Rev. 104*, 617–649.
9. Zheng, Z., and Gunner, M. R. (2009) Analysis of the electrochemistry of hemes with E_ms spanning 800 mV. *Proteins 75*, 719–734.
10. Banci, L., Bertini, I., Rosato, A., and Varani, G. (1999) Mitochondrial cytochromes *c*: a comparative analysis. *J. Biol. Inorg. Chem. 4*, 824–837.
11. Lojou, E., Cutruzzola, F., Tegoni, M., and Bianco, P. (2003) Electrochemical study of the intermolecular electron transfer to *Pseudomonas aeruginosa* cytochrome cd_1 nitrite reductase. *Electrochim. Acta 48*, 1055–1064.
12. Hengartner, M. O. (2000) The biochemistry of apoptosis. *Nature 407*, 770–776.
13. Li, P., Nijhawan, D., Budihardjo, I., Srinivasula, S. M., Ahmad, M., Alnemri, E. S., and Wang, X. D. (1997) Cytochrome *c* and dATP-dependent formation of Apaf-1/caspase-9 complex initiates an apoptotic protease cascade. *Cell 91*, 479–489.
14. Bianco, P., Haladjian, J., Pilard, R., and Bruscha, M. (1982) Electrochemistry of *c*-type cytochromes: Electrode reactions of cytochrome c_{553} from *Desulfovibrio vulgaris* Hildenborough. *J. Electroanal. Chem. 136*, 291–299.
15. Benini, S., Borsari, M., Ciurli, S., Dikiy, A., and Lemborghini, M. (1998) Modulation of *Bacillus pasteurii* cytochrome c_{553} reduction potential by structural and solution parameters. *J. Biol. Inorg. Chem. 3*, 371–382.
16. Springs, S. L., Bass, S. E., and McLendon, G. L. (2000) Cytochrome b_{562} Variants: A library for examining redox potential evolution. *Biochemistry 39*, 6075–6082.
17. Battistuzzi, G., Borsari, M., Cowan, J. A., Ranieri, A., and Sola, M. (2002) Control of cytochrome *c* redox potential: Axial ligation and protein environment effects. *J. Am. Chem. Soc. 124*, 5315–5324.
18. dos Santos, M. M. C., de Sousa, P. M. P., Goncalves, M. L. S., Krippahl, L., Moura, J. J. G., Lojou, E., and Bianco, P. (2003) Electrochemical studies on small electron transfer proteins using membrane electrodes. *J. Electroanal. Chem. 541*, 153–162.
19. Matsuura, Y., Takano, T., and Dickerson, R. E. (1982) Structure of cytochrome c_{551} from *Pseudomonas aeruginosa* refined at 1.6 Å resolution and comparison of the two redox forms. *J. Mol. Biol. 156*, 389–409.
20. Sanbongi, Y., Ishii, M., Igarashi, Y., and Kodama, T. (1989) Amino acid sequence of cytochrome *c*-552 from a thermophilic hydrogen-oxidizing bacterium *Hydrogenobacter thermophilus*. *J. Bacteriol. 171*, 65–69.
21. Travaglini-Allocatelli, C., Gianni, S., Dubey, V. K., Borgia, A., Di Matteo, A., Bonivento, D., Cutruzzola, F., Bren, K. L., and Brunori, M. (2005) An obligatory intermediate in the folding pathway of cytochrome c_{552} from *Hydrogenobacter thermophilus*. *J. Biol. Chem. 280*, 25729–25734.
22. Terui, N., Tachiiri, N., Matsuo, H., Hasegawa, J., Uchiyama, S., Kobayashi, Y., Igarashi, Y., Sambongi, Y., and Yamamoto, Y. (2003) Relationship between redox function and protein stability of cytochromes *c*. *J. Am. Chem. Soc. 125*, 13650–13651.
23. Takayama, S. J., Mikami, S., Terui, N., Mita, H., Hasegawa, J., Sambongi, Y., and Yamamoto, Y. (2005) Control of the redox potential of *Pseudomonas aeruginosa* cytochrome c_{551} through the Fe-Met coordination bond strength and pK_a of a buried heme propionic acid side-chain. *Biochemistry 44*, 5488–5494.
24. Takahashi, Y., Sasaki, H., Takayama, S. J., Mikami, S., Kawano, S., Mita, H., Sambongi, Y., and Yamamoto, Y. (2006) Further enhancement of the thermostability of *Hydrogenobacter thermophilus* cytochrome c_{552}. *Biochemistry 45*, 11005–11011.
25. Takahashi, Y., Takayama, S. J., Mikami, S., Mita, H., Sambongi, Y., and Yamamoto, Y. (2006) Influence of a single amide group on the redox function of *Pseudomonas aeruginosa* cytochrome c_{551}. *Chem. Lett. 35*, 528–529.
26. Battistuzzi, G., Borsari, M., Sola, M., and Francia, F. (1997) Redox thermodynamics of the native and alkaline forms of eukaryotic and bacterial class I cytochromes *c*. *Biochemistry 36*, 16247–16258.
27. Tezcan, F. A., Winkler, J. R., and Gray, H. B. (1998) Effects of ligation and folding on reduction potentials of heme proteins. *J. Am. Chem. Soc. 120*, 13383–13388.
28. Banci, L., Bertini, I., Huber, J. G., Spyroulias, G. A., and Turano, P. (1999) Solution structure of reduced horse heart cytochrome *c*. *J. Biol. Inorg. Chem. 4*, 21–31.
29. Battistuzzi, G., Borsari, M., Ronieri, A., and Sola, M. (2004) Solvent-based deuterium isotope effects on the redox thermodynamics of cytochrome *c*. *J. Biol. Inorg. Chem. 9*, 781–781.
30. Moore, G. R., Pettigrew, G. W., Pitt, R. C., and Williams, R. J. P. (1980) pH dependence of the redox potential of *Pseudomonas aeruginosa* cytochrome *c*-551. *Biochim. Biophys. Acta 590*, 261–271.
31. Moore, G. R. (1983) Control of redox properties of cytochrome *c* by special electrostatic interactions. *FEBS Lett. 161*, 171–175.

32. Leitch, F. A., Moore, G. R., and Pettigrew, G. W. (1984) Structural basis for the variation of pH-dependent redox potentials of *Pseudomonas* cytochromes *c*-551. *Biochemistry 23*, 1831–1838.
33. Hasegawa, J., Shimahara, H., Mizutani, M., Uchiyama, S., Arai, H., Ishii, M., Kobayashi, Y., Ferguson, S. J., Sambongi, Y., and Igarashi, Y. (1999) Stabilization of *Pseudomonas aeruginosa* cytochrome c_{551} by systematic amino acid substitutions based on the structure of thermophilic *Hydrogenobacter thermophilus* cytochrome c_{552}. *J. Biol. Chem. 274*, 37533–37537.
34. Hasegawa, J., Uchiyama, S., Tanimoto, Y., Mizutani, M., Kobayashi, Y., Sambongi, Y., and Igarashi, Y. (2000) Selected mutations in a mesophilic cytochrome *c* confer the stability of a thermophilic counterpart. *J. Biol. Chem. 275*, 37824–37828.
35. Taniguchi, I., Iseki, M., Eto, T., Toyosawa, H., Yamaguchi, H., and Yasukouchi, K. (1984) The effect of pH on the temperature dependence of the redox potential of horse heart cytochrome *c* at a bis(4-pyridyl)disulfide-modified gold electrode. *Bioelectrochem. Bioenerg. 13*, 373–383.
36. Ueyama, S., Isoda, S., Hatanaka, H., and Shibano, Y. (1996) Macroscopically rapid electron transfer of cytochrome c_{522} with high thermostability at bare and surface-modified gold electrodes. *J. Electroanal. Chem. 401*, 227–230.
37. Cuttruzzolá, F., Arese, M., Ranghino, G., van Pouderroyen, G., Canters, G., and Brunori, M. (2002) *Pseudomonas aeruginosa* cytochrome c_{551}: probing the role of the hydrophobic patch in electron transfer. *J. Inorg. Biochem. 88*, 353–361.
38. Clark, W. K. (1960) Oxidation reduction potentials of organic systems, Williams & Wilkins, Baltimore, MD.
39. Uchiyama, S., Hasegawa, J., Tanimoto, Y., Moriguchi, H., Mizutani, M., Igarashi, Y., Sambongi, Y., and Kobayashi, Y. (2002) Thermodynamic characterization of variants of mesophilic cytochrome *c* and its thermophilic counterpart. *Protein Eng. 15*, 455–461.
40. La Mar, G. N., Satterlee, J. D., and de Ropp, J. S. (2000) Nuclear magnetic resonance of hemoproteins, in The porphyrin handbook (Kadish, K., Smith, K. M., and Guilard, R., Eds.) pp 185−298, Academic Press, New York.
41. Bertini, I., and Luchinat, C. (1986) NMR of paramagnetic molecules in biological systems, pp 19−46, Benjamin/Cummings Publishing Co., Menlo Park, CA.
42. Yamamoto, Y. (1998) NMR study of active sites in paramagnetic hemoproteins. *Annu. Rep. NMR Spectrosc. 36*, 1–77.
43. Dutton, P. L. (1978) Redox potentiometry: determination of midpoint potentials of oxidation-reduction components of biological electron-transfer systems. *Methods Enzymol. 54*, 411–434.
44. Simonson, T., Carlsson, J., and Case, D. A. (2004) Proton binding to proteins: pK_a calculations with explicit and implicit solvent models. *J. Am. Chem. Soc. 126*, 4167–4180.
45. Battistuzzi, G., Borsari, M., Ronieri, A., and Sola, M. (2002) Conservation of the free energy change of the alkaline isomerization in mitochondorial and bacterial cytochromes *c*. *Arch. Biochem. Biophys. 404*, 227–233.
46. Battistuzzi, G., Borsari, M., Di Rocco, G., Ronieri, A., and Sola, M. (2004) Enthalpy/entropy compensation phenomena in the reduction thermodynamics of electron transport metalloproteins. *J. Biol. Inorg. Chem. 9*, 23–26.
47. Battistuzzi, G., Borsari, M., Dallari, D., Lancellotti, I., and Sola, M. (1996) Anion binding to mitochondrial cytochrome *c* studied through electrochemistry. Effects of the neutralization of surface charges on the redox potential. *Eur. J. Biochem. 241*, 208–214.